Multilevel MDA-Lite Paris Traceroute

Kevin Vermeulen
Sorbonne Université

Stephen D. Strowes
RIPE NCC

Olivier Fourmaux
Sorbonne Université

Timur Friedman
Sorbonne Université

ABSTRACT

Since its introduction in 2006-2007, Paris Traceroute and its Multipath Detection Algorithm (MDA) have been used to conduct well over a billion IP level multipath route traces from platforms such as M-Lab. Unfortunately, the MDA requires a large number of packets in order to trace an entire topology of load balanced paths between a source and a destination, which makes it undesirable for platforms that otherwise deploy Paris Traceroute, such as RIPE Atlas. In this paper we present a major update to the Paris Traceroute tool. Our contributions are: (1) MDA-Lite, an alternative to the MDA that significantly cuts overhead while maintaining a low failure probability; (2) Fakeroute, a simulator that enables validation of a multipath route tracing tool's adherence to its claimed failure probability bounds; (3) multilevel multipath route tracing, with, for the first time, a Traceroute tool that provides a router-level view of multipath routes; and (4) surveys at both the IP and router levels of multipath routing in the Internet, showing, among other things, that load balancing topologies have increased in size well beyond what has been previously reported as recently as 2016. The data and the software underlying these results are publicly available.

CCS CONCEPTS

• **Networks → Network measurement**; **Network monitoring**; *Topology analysis and generation*;

KEYWORDS

Active Internet Measurements; Traceroute, Alias Resolution

1 INTRODUCTION

Since its introduction by Van Jacobson in 1988 [31], Traceroute has become ubiquitous on both end-systems and routers for tracing forward paths through the Internet between source and destination at the IP level. Network operators use it for troubleshooting; the network measurement community uses it in its studies; and vast numbers of route traces are executed daily by long term Internet survey infrastructure such as Ark [1], M-Lab [9, 25], and RIPE

Atlas [11, 40]. Two updates were proposed to Traceroute in 2006-2007 to take into account the ever-increasing presence of load balancing routers: the Paris technique [15, 48], for tracing a single clean path through load balancers, and the Multipath Detection Algorithm (MDA) [17, 47], for discovering all of the load balanced paths at the IP level between source and destination. Well over a billion route traces using the MDA have been executed by Ark and M-Lab [23] in the intervening years, and the Paris technique is used for route tracing on the over 10,000 RIPE Atlas probes.

A disincentive to deploying the MDA is the network overhead that it requires. By way of example, suppose a given hop in a route being traced is evenly load balanced across two interfaces. If the MDA were to match the overhead of a typical command line Traceroute tool and send just three probes per hop, the first probe will find one interface and the subsequent two probes will together have a 25% probability of missing the other interface. In order to bring the probability of failing to discover both interfaces under 1%, a total of eight probes would need to be sent to that hop. Even for a single load balanced hop, we must more than double the workload. To have a high degree of confidence in full discovery of full load balanced topologies requires hundreds or even thousands of packets. Our work is motivated by the aim of minimising this overhead.

This paper makes four contributions that advance the state of the art for multipath route tracing in the IPv4 Internet. First is *MDA-Lite* (Sec. 2), a lower overhead alternative to the MDA that is tailored to the most common load balanced topologies that we encounter in the Internet. We identify a characteristic that we call "diamond uniformity" that often holds and that can permit significant probe savings. Second is *Fakeroute* (Sec. 3), which validates, to a high degree of confidence, that a software tool's implementation of its multipath route detection algorithm performs as intended on a variety of simulated test topologies. Third is *Multilevel MDA-Lite Paris Traceroute* (Sec. 4), which, for the first time, integrates router-level view of multipath routes, into a Traceroute tool. Until now this has only been done by other tools once route tracing is complete. Fourth, we provide *new survey results* (Sec. 5) for multipath routing in the Internet, both at the IP level, and at the router level. We report load balancing practices on a scale (up to 96 interfaces at a single hop) never before described.

Both our code and our survey results are publicly available at `https://gitlab.planet-lab.eu/cartography/`.

2 MDA-LITE

The idea behind the MDA-Lite is that we can take advantage of prior knowledge of what a route trace is likely to encounter in order to probe more efficiently. Experience tells us, and our survey in Sec. 5.1 confirms, that some multipath route patterns are frequently

encountered in the Internet, whereas others are not. The MDA-Lite algorithm operates on the assumption that a topological feature that we call "uniformity" will be prevalent and that another feature that we call "meshing" will be uncommon. It includes tests to detect deviations from these assumptions. We detail these two topological features in Sec. 2.2.

2.1 The MDA and possible probe savings

This section recalls how the MDA works, stepping us through examples of the discovery of what are called "diamonds", as shown in Fig. 1. We see how a feature of the algorithm that we dub "node control" requires large numbers of probes to be sent.

The MDA has evolved through 2006 and 2007 poster and workshop versions [16, 18] to its present form in an Infocom 2009 paper [47]. This latter publication describes an idealized formal model for multipath route discovery [47, Sec. II.A], based upon a set of assumptions about the Internet, and explains the adaptations made [47, Sec. III.A], in crafting the MDA, to accommodate some divergences assumptions and reality. These assumptions are: "(1) No routing changes during the discovery process. [...] (2) There is no per-packet load balancing. (As a result, we can manipulate a probe packet's flow identifier to cause it to pass through a chosen node.) (3) Load balancing is uniform-at-random across successor nodes. (4) All probes receive a response. (5) The effect of sending one probe packet has no bearing on the result of any subsequent probe. In particular, load balancers act independently."

The MDA works on the basis of an *open set* of vertices [47, Sec. II.A], each of which has been discovered but has not yet had its successor vertices identified. A discovery round consists in choosing a vertex v from the open set and trying to find all of its successors. Where there is no load balancing, v has just one successor, but if v is the responding interface of a load balancing router, there will be two or more possible successors that can only be identified by stochastic probing. In the case that concerns us, per-flow load balancing, successors are found by varying the flow identifier from one probe packet to the next. An extension [17, Sec. 3.2], that we do not employ here, would allow us to measure per-destination load balancing, the effects of which are identical to routing insofar as a single destination is concerned.

The number of probe packets the MDA sends to discover all successors of a vertex v is governed by a set of predetermined stopping points, designated n_k. If k successors to v have been discovered then the MDA keeps sending probes until either the number of probes equals n_k or an additional successor has been discovered. In the latter case, the new stopping point becomes n_{k+1}. Eventually, one of the stopping points will be reached. The stopping points are set in such a way as to guarantee that the probability of failing to discover all of the successors of a given vertex is bounded. Combined with the assumption of a maximum number of branching points, this implies a bound on the failure to discover an entire topology. The MDA takes as a tunable parameter this global failure probability bound and works backwards to calculate the failure bound on discovering all the successors to a given vertex, which in turn determines the values n_k.

Diamond: As defined by Augustin et al. [19], a *diamond* is "a subgraph delimited by a divergence point followed, two or more

hops later, by a convergence point, with the requirement that all flows from source to destination flow through both points". Fig. 1 provides examples of the MDA successfully discovering the full topologies of two similar diamonds: each one has a divergence point at hop 1, followed by four vertices at hop 2, two vertices at hop 3, and a convergence point at hop 4. Each vertex represents an IP interface, which is to say that these are IP level graphs, not router-level graphs. The full diamonds are shown at steps 4 and 4′ in the figure. We call the one at step 4 an "unmeshed" diamond and the one at step 4′ "meshed", the difference relating to the links between hops 2 and 3. Sec. 2.2 provides a formal definition of meshing. Since discovery is identical for hops 1 and 2, we show the first two steps for the unmeshed diamond and do not repeat them for the meshed one. A vertex at hop 2 of the unmeshed diamond is highlighted and two hypothetical successors are shown in order to illustrate "node control", a concept described below.

Hop 1: The MDA sends a probe that discovers the single vertex at hop 1. It continues by sending additional probes to that hop, each with a different flow ID, until it reaches the stopping point of n_1 probes, at which point it rules out the existence of a second vertex at that hop. The annotation shows a total of n_1 probes having been sent to hop 1.

Hop 2: The MDA sends a probe that discovers a vertex at hop 2. As with hop 1, it sends additional probes, each with a different flow ID, but in this example it discovers a second vertex on or before having sent n_1 probes. Thus the limit becomes n_2. Third and fourth vertices are discovered before n_2 and n_3, respectively, are met. When n_4 is reached, no fifth vertex has been found and so the MDA stops scanning this hop.

Node control: When a hop has more than one vertex, the MDA works on the hypothesis that each of these vertices is a potential divergence point with successors that are perhaps reachable only via that vertex. It therefore employs what we dub here *node control*, which ensures that each probe packet that goes to the subsequent hop does so via the chosen vertex.

We have illustrated node control with the highlighted vertex at hop 2, and the hypothesis that it has two successor vertices at hop 3. The MDA needs to identify a minimum of n_1 flow IDs that bring probes having a TTL of 2 to the highlighted vertex in order to send probes to TTL 3 via that vertex. In order to exercise node control for each of the four vertices at hop 2, a minimum of $4n_1$ probes must be sent to hop 2. Depending upon the specific stopping point values, it can be unlikely or even impossible for the n_4 probes that had initially discovered the vertices at hop 2 to have resulted in at least n_1 of them reaching each of the four vertices. To take a numerical example from Veitch et al.'s Table 1 [47, Sec. III.B], $n_1 = 9$ and $n_4 = 33$. In this case, it is impossible for the 33 probes that were used in hop 2 discovery to yield 9 flow IDs for each of hop 2's four vertices; at least $4 \times 9 = 36$ probes would be required for that. 36 probes are unlikely to be distributed perfectly evenly, so some additional probing is necessary. The annotation at hop 2 is updated in the illustration for hop 3 to indicate that $4n_1 + \delta$ probes have been sent to hop 2, where δ is a non-negative integer.

The node control problem is an instance of the Multiple Coupon Collector's problem, which is described by Newman et al. [38] and more recently by Ferrante et al. [26].
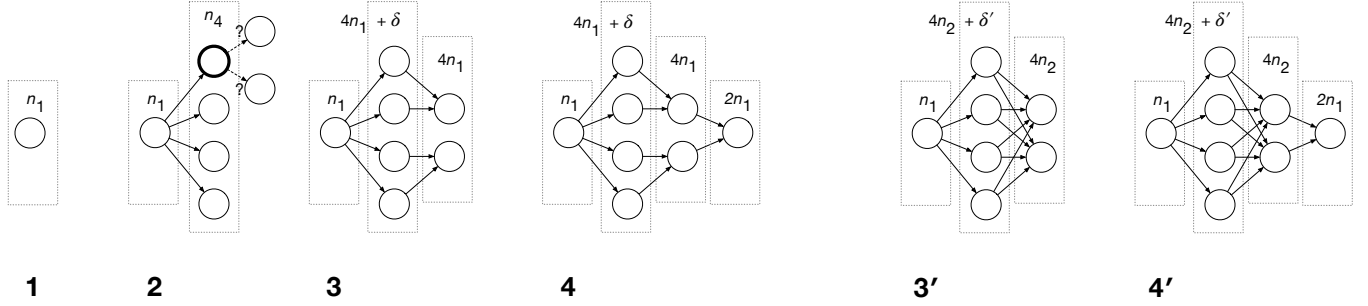
Figure 1: MDA discovery of an unmeshed and a meshed diamond

Hop 3: Having generated the flow IDs necessary for node control, the MDA now sends probes to hop 3: n_1 probes via each of the four hop 2 vertices. For the unmeshed topology in this example, only one successor vertex is discovered for each hop 2 vertex. The annotation shows a total of $4n_1$ probes having been sent to hop 3.

Hop 4: The MDA also exercises node control at hop 3 in order to probe hop 4. In this example, since n_1 probes have already reached each hop 3 vertex, no further flow IDs need to be generated. The annotation shows a total of $2n_1$ probes having been sent to hop 4, where the diamond's convergence point is discovered.

A total of $11n_1 + \delta$ probes will have been sent overall to discover this topology. Using the values from Veitch et al., $99 + \delta$ probes will have been required by the MDA. The values from Veitch et al. illustrate the cost of node control: $4n_1 = 36$ probes were sent to hop 3, whereas only $n_2 = 17$ probes were strictly necessary at that hop, and twice as many probes than necessary were sent to hop 4.

Hop 2 node control under meshing: The numbers differ for the meshed diamond starting at the third hop, which we distinguish in Fig. 1 with the label 3′. Each hop 2 vertex has two successors at hop 3′, as opposed to just one at hop 3. Presuming the MDA discovers the second successor in each case, node control requires additional probes to be sent to hop 2 such that there are at least n_2 flow IDs that reach each vertex at that hop. The annotation shows a total of $4n_2 + \delta'$ probes having been sent to hop 2 for the meshed diamond.

Hop 3′: As the annotation shows, a total of $4n_2$ probes are sent to hop 3′. The meshing results in more probes than the $4n_1$ probes sent to hop 3 in the unmeshed diamond.

Hop 4′: There being only one node at hop 4′, the annotation shows a total of $2n_1$ robes are sent to that hop, just as for hop 4 in the unmeshed diamond.

A total of $8n_2 + 3n_1 + \delta'$ probes will have been sent overall to discover the meshed topology. Using the values from Veitch et al., $163 + \delta'$ probes will have been required by the MDA. Again, we see the cost of node control, here accentuated by the multiple successors to each hop 2 vertex.

Per-packet load balancing: Since per-packet load balancing was found to be rare in Augustin et al.'s 2011 survey [19], we consider that the assumption (2) of no per-packet load balancing described at the start of this subsection is a reasonably good one, and we have omitted the additional packets to check for per-packet load balancing from our implementation of the MDA, as well as from the MDA-Lite.

2.2 Uniformity and meshing

As we see in the Fig. 1 examples, the MDA's use of node control is costly in the number of probes that it requires. However, node control is only necessary for certain kinds of diamonds, which we describe here. If diamonds that require node control are sufficiently rare, an "MDA-Lite" could do away with much of the need for node control. As we shall see, a small degree of node control is still required in order to determine which sort of diamond has been encountered. When necessary, the MDA-Lite can switch over to the MDA with full node control.

We have identified a diamond feature that we call "uniformity" that allows full topology discovery without node control. We have also identified a characteristic of diamonds that we call "meshing" that counteracts the potential for probe savings that uniformity otherwise offers. We define uniformity and meshing here and, as we show in Sec. 5.1, uniform unmeshed diamonds are indeed very common. Therefore, probe savings can be realized by using the MDA-Lite.

Uniformity: We define a *uniform hop* as one at which there is an equal probability for each of its vertices to be reached by a probe with that hop's TTL and a randomly chosen flow identifier. For a uniform hop, the failure probability bounds associated with the MDA's stopping points, the values n_k, apply to discovery of all the vertices at a hop, and node control is not required. A diamond as a whole is considered a *uniform diamond* if all of its hops are uniform.

Meshing: As already implied, meshing has to do with the links between adjacent hops. Consider hops at TTLs i and $i+1$. We define these to be *meshed hops* if one of the three following conditions applies:

- The hops have identical numbers of vertices and the out-degree of at least one of the vertices at hop i is two or more. Equivalently, the in-degree of at least one of the vertices at hop $i + 1$ is two or more.
- Hop i has fewer vertices than hop $i + 1$ and the in-degree of at least one of the vertices at hop $i + 1$ is two or more.
- Hop i has more vertices than hop $i + 1$ and the out-degree of at least one of the vertices at hop i is two or more.

We define a *meshed diamond* as a diamond with at least one pair of meshed hops. The right-hand side of Fig. 6 illustrates a meshed diamond, in which hop pairs $(2, 3)$ and $(4, 5)$ are meshed.

2.3 The MDA-Lite algorithm

The MDA proceeds vertex by vertex, employing node control to seek the successors to each vertex individually. The MDA-Lite, however, reserves node control for particular cases and proceeds hop by hop in the general case. At each hop it seeks to discover all of the vertices at that hop, and in doing so discovers some portion of the edges between that hop and the prior hop. It then seeks out the remaining edges. It operates on the assumption that the diamonds that it encounters will be uniform and unmeshed. If this assumption holds, hop-by-hop probing will maintain the MDA's failure probability bounds. Because these two topology assumptions might not hold, the MDA-Lite tests for a lack of uniformity and the presence of meshing using methods that are less costly than full application of the MDA. When it detects a diamond that does not adhere to one of the assumptions, it switches to the MDA. These steps are described below.

2.3.1 Uniform, unmeshed diamonds. The MDA-Lite, operating on the assumption that a hop is uniform, sends probes to that hop without node control. It starts by reusing one flow identifier from each of the vertices that it has discovered at the previous hop, continuing with additional previously-used flow identifiers and then new ones. It applies the MDA's stopping rule to remain within the MDA's failure probability bounds for vertex detection.

To take as examples the topologies in Fig. 1, the MDA-Lite sends n_4 probes to hop 2, n_2 probes to hop 3, and n_1 probes to hop 4. Discovery of all vertices in the diamond therefore requires $n_4 + n_2 + 2n_1$ probes, or 68 probes when applying the values in Veitch et al.'s Table 1, regardless of whether the diamond is unmeshed or meshed. This compares to the numbers for the MDA that we determined above: $99 + \delta$ probes for the unmeshed diamond and $163 + \delta'$ probes for the meshed diamond.

Discovering all of the vertices at adjacent hops i and $i + 1$ does not imply that the MDA-Lite will have discovered all of the edges. Finishing up the edge discovery is straightforward, though, for unmeshed hops, in the sense that it is deterministic rather than stochastic. It consists of tracing backward from each vertex at hop $i+1$ that does not yet have an identified predecessor or forward from each vertex at hop i that does not yet have an identified successor. There are three cases to consider:

- Hop $i + 1$ has fewer vertices than hop i. For each hop i vertex that does not yet have an identified successor, the flow identifier of a probe that has discovered that vertex is used to send a probe to hop $i + 1$. Assuming no meshing, this completes the edge discovery.
- Hop $i + 1$ has more vertices than hop i. For each vertex at hop $i + 1$ that does not yet have an identified predecessor, the flow identifier of a probe that has discovered that vertex is used to send a probe to hop i. Assuming no meshing, this completes the edge discovery.
- Hop $i + 1$ has the same number of vertices as hop i. We apply both of the methods just explained above.

Because a diamond could be meshed or non-uniform, the MDA-Lite tries to detect those cases, as described below.

2.3.2 Detecting meshing. To detect meshing, stochastic probing is required, and this involves a limited application of node control.

For a pair of hops having two or more vertices each, the meshing test consists of tracing from the hop with the greater number of vertices to the one with the lesser number of vertices, or tracing in either direction if the hops have equal numbers of vertices. When tracing forwards, meshing is detected if any predecessor vertex has an out-degree of 2 or more. For backwards tracing, it is if any successor vertex has an in-degree of 2 or more. The test requires node control: We introduce a parameter, $\phi \geqslant 2$, for the MDA-Lite, which determines the number of flow identifiers that have to be generated for each vertex at the hop from which tracing will begin. Probes with these flow IDs are sent to the other hop.

The probability of failing to detect meshing depends upon ϕ. We calculate this probability as follows. Suppose that the test is through forward tracing, and let V be the set of two or more vertices at hop i and let $\sigma(v)$ designate the set of successor nodes of a vertex $v \in V$. When ϕ flow IDs are generated for each vertex $v \in V$ and probes with those flow identifiers are sent to hop $i + 1$, the probability of failing to detect meshing is:

$$\prod_{v \in V} \frac{1}{|\sigma(v)|^{\phi-1}} \tag{1}$$

This probability calculation extends with trivial adjustments to the case of backward tracing.

A minimum value $\phi = 2$ is required in order to detect meshing. Whether to use a higher value, with a lower failure probability, is up to the MDA-Lite implementation. We examined how well this minimum value would work on the meshed diamonds identified by the MDA in the survey that is described in Sec. 5.1. Looking at the topology of each hop pair, we calculated the probability of the MDA-Lite failing to detect the meshing. We did this both for *measured diamonds*, which is to say that each diamond is weighted by the number of times that it is encountered in the survey, and for *distinct diamonds*, in which we weight each diamond just once, regardless of how many times it has been seen. Fig. 2 plots CDFs for the probability of the MDA-Lite with $\phi = 2$ missing meshing at a hop pair for which the MDA detected meshing. We see that,

(a) Measured   (b) Distinct
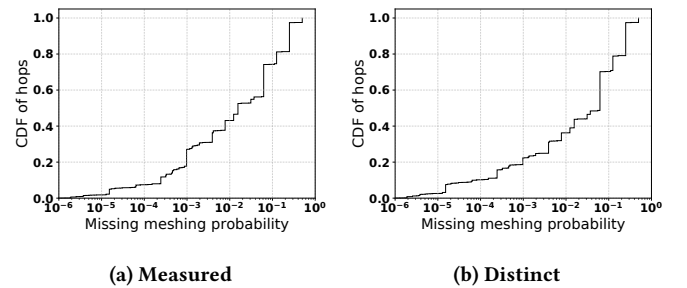
Figure 2: The probability of failing to detect meshing

for both measured and distinct diamonds, the probability of failing to detect meshing is 0.1 or less on 70% of meshed hop pairs and 0.25 or less on 95% of the cases. If we consider this to be too high a probability, ϕ is tunable, and we can set it to 3 or 4.

The overhead generated by the meshing test is lower than the overhead of the MDA's use of node control. Even with a value of ϕ of 3 or 4, this is lower than $n_1 = 9$, the minimum number of flow identifiers per vertex required by the MDA's use of node control in

Veitch et al.. Furthermore, the MDA-Lite's meshing test is applied only to a minority of diamonds. As previous surveys have shown, and our survey confirms, nearly half of all diamonds consist of only a single multi-vertex hop (48% for measured and 45% for distinct diamonds). The MDA-Lite's meshing test only applies where there are two adjacent multi-vertex hops, but the MDA applies node control whenever there is a multi-vertex hop.

2.3.3 Detecting non-uniformity. Once edge discovery is complete, and if the MDA has not been engaged because of meshing, the MDA-Lite tests for non-uniformity. The test is a purely topological one because the MDA-Lite makes the same assumption as the MDA about the evenness of load balancing: that each load balancer dispatches flow IDs in a uniform manner. (Based upon our experience, this appears to be a realistic assumption, but a survey on this particular point would be worthwhile.) What we term "width asymmetry" in our survey (see Sec. 5) is therefore the indicator of non-uniformity.

The MDA-Lite detects width asymmetry as follows. For a pair of hops i and $i+1$, if the number of successors is not identical for every vertex at hop i or if the number of predecessors is not identical for every vertex at hop $i+1$, the diamond has width asymmetry and is considered to be non-uniform, and the MDA-Lite switches over to the MDA.

Finding non-uniformity depends upon the topology in question having been fully revealed. Unlike the MDA, the MDA-Lite does not provide statistical guarantees on full topology discovery. Rather, the MDA-Lite assumes that any non-uniformity is likely to be low so that the full topology will most probably be revealed. We empirically justify this assumption based upon our survey results in Sec. 5.1.

2.4 MDA-Lite evaluation

We have tested the MDA-Lite both through simulations and measurements on the Internet, finding in both cases that it compares favorably to the full MDA.

2.4.1 Evaluation through simulations. Simulations allow us to compare the MDA-Lite to the MDA on known topologies and in an environment free of factors, such as variations in router load, that are not related to the algorithms. We have chosen topologies based on both the categories of diamond that are relevant to the MDA-Lite (uniform or asymmetric, meshed or not, see Sec. 2.3), and on what we found in our survey (Sec. 5.1).

- The *max length 2 diamond*, found on the trace pl2.prakinf.-tu-ilmenau.de to 83.167.65.184, consists of a divergence point, a 28 vertex hop, and a convergence point. Nearly half of all diamonds in the survey are of maximum length 2, though this is a particularly wide example. Where the MDA will perform node control on each of the 28 vertices, the MDA-Lite will avoid doing so. Finding no adjacent multi-vertex hops, the MDA-Lite will not apply its meshing test.
- The *symmetric diamond*, found on the trace ple1.cesnet.cz to 203.195.189.3, has three multi-vertex hops, with 10 being the most vertices at a hop. There is no meshing between the hops. On this diamond, the MDA-Lite will be obliged to perform a light version of node control in order to test
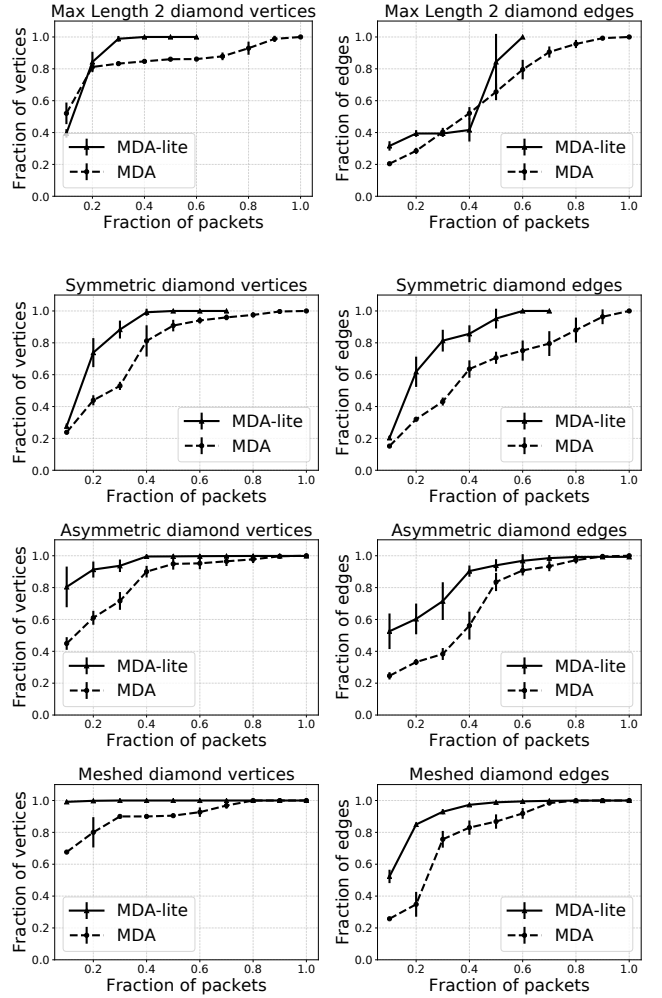
Figure 3: MDA-Lite versus MDA simulations

for meshing. Finding none, it will not switch over to the full MDA.

- The *asymmetric diamond*, found on the trace kulcha.mimuw.-edu.pl to 61.6.250.1, has nine multi-vertex hops, with 19 being the most vertices at a hop. The edges are laid out in such a way that at least one of the hops is not uniform, which is to say that there is a greater probability of a probe packet with an arbitrarily chosen flow identifier reaching some vertices at that hop rather than others. It has a "width asymmetry" of 17 (this metric is defined in Sec. 5). It is unmeshed. If the MDA-Lite discovers the asymmetry, it will be obliged to switch over to the full MDA.
- The *meshed diamond*, found on the trace ple2.planetlab.eu to 125.155.82.17, has five multi-vertex hops, with 48 being the most vertices at a hop. It is meshed, and if the MDA-Lite discovers the meshing it will be obliged to switch over to the full MDA.

The simulations ran on Fakeroute, the tool that we describe in Sec. 3. Fig. 3 shows the results of 30 runs on each of the four topologies, with vertex discovery graphs on the left and edge discovery graphs

on the right. Two curves are plotted on each graph: one for the MDA-Lite with $\phi = 2$ and one for the MDA. The portion of the topologies' vertices or edges discovered as each algorithm is running is plotted on the vertical axis. The horizontal axis indicates the number of probe packets sent, normalized to 1.0 being the number of packets sent by the MDA in a given run. Since the MDA-Lite sends fewer packets when confronted with max length 2 and symmetric diamonds, its curves stop before reaching the right hand side of the graph. Error bars are given. We see that the MDA-Lite tends to discover more of these topologies faster than the MDA, though not always, and that it discovers the entire topology sooner. In cases where it does not need to switch over to the full MDA, it also economizes on the number of probes that it sends, reducing by 40% the full MDA's overhead on these examples. For these cases, we see that the MDA-Lite is not sacrificing the ability to discover the full topology. Because it is more economical in its use of probes, it discovers more faster. When it does not have to switch over to the full MDA, it uses significantly fewer probes. In the other cases, although it discovers the full topology faster than the MDA, the switch to the full MDA means no economy in its use of probes.

2.4.2 Evaluation through measurements. We performed our measurement-based evaluation on a sample of 10,000 source-destination pairs from our survey (Sec. 5.1) for which diamonds had been discovered. For each of these, we ran five variants of Paris Traceroute successively: two with the MDA; one with the MDA-Lite and $\phi = 2$; one with the MDA-Lite and $\phi = 4$; and one with just a single flow ID, the way Paris Traceroute is currently implemented on the RIPE Atlas infrastructure (Sec. 6.2). As a reminder, the parameter ϕ, defined in Sec. 2.3.2, governs how much effort the MDA-Lite will expend in trying to detect meshing.

For each topology, the first run with the MDA serves as the basis for comparing the other algorithms. We calculate the ratio of vertices discovered, edges discovered, and packets sent. The results, plotted as CDFs, are shown in Fig. 4. The horizontal axis plots the ratios in log scale, with 10^0 indicating that the algorithms performed the same. For the vertex and edge discovery plots, a value to the left of this value indicates that the competing algorithm discovered less than the first MDA run, and so performed worse, and a value to the right indicates that it discovered more, and so performed better. For the packets plot, at 1, the tools sent the same number of packets, whereas a value to the left of this indicates that the competing algorithm sent fewer packets than the first MDA run, and so performed better, whereas a value to the right of this indicates that the competing algorithm sent more packets than the first MDA run, and so performed worse.

We run the MDA algorithm twice because there are variations from run to run, both because of changing network conditions and because of the stochastic nature of MDA and MDA-Lite discovery. The second MDA will sometimes perform better, sometimes worse than the first, and its curve, shown as a solid black line in the plots, forms the basis against which to compare the other algorithms. While the second MDA performs close to the first, it discovers fewer vertices 12% of the time and more vertices 12% of the time; fewer edges 20% of the time and more edges 20% of the time. We believe that these differences are largely attributable to the stochastic nature of the MDA, meaning that either the first

	Vertices	Edges	Packets
MDA 2	0.998	0.999	1.005
MDA-Lite $\phi = 2$	1.002	1.007	0.696
MDA-Lite $\phi = 4$	1.004	1.005	0.711
Single flow ID	0.537	0.201	0.040

Table 1: Comparative performance on aggregated topology: ratios with respect to a first MDA round over 10,000 measurements in the Internet

or the second run occasionally terminates its discovery process without having discovered all of the vertices (and hence edges) that are available to discover. Recall from Sec. 2 that the MDA's failure bound for discovering the successors to a vertex is set as a function of a global failure bound for the entire topology and a maximum number of branching points that the topology might have. This latter parameter is set to 30 by default, but in complex topologies of the sort that we have encountered in our survey, there can be far more branching points.

For the comparison between the MDA and the MDA-Lite, we observe that there is no discernible difference between $\phi = 2$ and $\phi = 4$ for the MDA-Lite. Most importantly, the MDA-Lite performs nearly identically to the second MDA run with respect to the first MDA run: sometimes better, sometimes worse. Compared to the first MDA run, the MDA-Lite performed better 14% of the time and worse 14% of the time for the vertices; better 20% of the time and worse 26% of the time for the edges. We attribute the larger number of instances of worse performance to the occasional failure of MDA-Lite to detect meshing or non-uniformity. The impact of this greater number on overall performance is negligible, as the ratio curves are hard to distinguish.

Paris Traceroute with a single flow ID performs notably worse on the whole than the MDA in both vertex and edge discovery. In only 12% of the cases, we observed at least 90% of the vertices and in only 10% of the cases, we observed at least 90% of the edges. We did detect some outliers where Paris Traceroute with a single flow ID discovers a greater number of vertices and edges than the MDA. These correspond, we believe, to cases where the route changed between the runs.

The other aspect of performance that concerns us is the number of packets that were sent. In 89% of the comparisons, the MDA-Lite realized probe savings. We find that we save 40% of the probes on 30% of the topologies. The ratio curves for both $\phi = 2$ and $\phi = 4$ are nearly identical and they are clearly superior to the curve for the second MDA run, meaning that when there is a diamond in the topology, the MDA-Lite will tend to use significantly fewer packets that the MDA.

Paris Traceroute with a single flow ID sends many fewer packets. The cost of discovering an entire multipath topology via the MDA can be anywhere from less than 2 times more to 1000 times more than the cost of tracing a single route with a single flow ID.

From a macroscopic point of view, Table 1 provides results on the overall topology formed by the aggregation of the 10,000 measurements of the evaluation dataset. Ratios of topology discovered and probes sent are computed with respect to the first MDA. We see that the topologies discovered by the MDA and the MDA-Lite
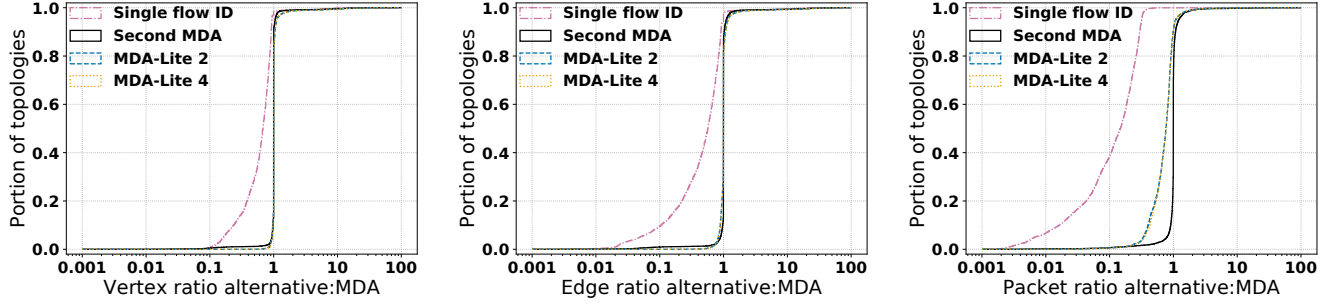
Figure 4: Comparative performance: CDFs over 10,000 measurements in the Internet

are very close, with a maximum of 0.7% difference for the edges. We see also that the MDA-Lite cuts the number of probe packets sent by roughly 30%. Paris Traceroute with a single flow ID sends only 4% of the packets sent by the first MDA, but only discovers 53.7% of the vertices and 20.1% of the edges.

3 FAKEROUTE

For any given multipath route between source and destination, one can calculate the precise probability of the MDA failing to detect the entire topology. This calculation is a simple application of the MDA's stopping rule with the chosen stopping points, the values n_k described in Sec. 2.1, along with the basic assumptions underlying the MDA, such as that load balancing will be uniform at random across successor vertices [47, Sec. II.A]. For a vertex in the topology that has $K > 1$ successors, the first successor will certainly be found by the first probe packet (among the assumptions is that all probes receive replies), but there is a probability $1/K^{n_1-1}$ that a total of n_1 probes will fail to discover a second successor, and the probabilities of failing to discover each of the remaining successors $k \leqslant K$ are similarly straightforward to calculate. Veitch et al. provide the details [47, Sec. II.B].

In principle, therefore, it should be possible to test that the MDA has been correctly implemented by a software tool by running it repeatedly on a suite of benchmark topologies and seeing that the failure probabilities are as predicted. For scientific purposes, we would want, if at all possible, to verify the conformance of a tool before using it, but we have not had that capability until now for tools that implement the MDA. Our contribution is a network multipath topology simulator that takes as input a given topology and a number of values n_k that is at least equal to the highest branching factor encountered in the topology, that calculates the probability that the MDA will fail to discover the full topology, and that runs the actual software tool in question repeatedly on the topology to verify that the tool does indeed fail at the predicted rate, not more, not less, providing a confidence interval for this result.

Our Fakeroute is a complete rewrite of the Fakeroute tool that has been provided as part of the *libparistraceroute* library [7], and which enabled small numbers of runs of a tool on a simulated topology, for simple debugging purposes, but that was not designed for large numbers of runs with statistical validation. The new Fakeroute, written in C++, uses *libnetfilter-queue* [6] to sniff probe packets

sent by a tool and suck them into the simulated environment rather than letting them out of the host into Internet. Once a probe is in, Fakeroute uses *libtins* [8] to read the flow identifier and TTL from its header fields. These are used to simulate the probe's passage through the topology, with the pseudo randomness of load balancing being emulated by the Mersenne Twister [2] that comes with the standard C++ library. Using *libtins*, Fakeroute crafts either an ICMP Time Exceeded or an ICMP Port Unreachable reply depending on whether the probe is determined to have reached an intermediate router or the destination, and sends that back to the tool. For example, on a topology with the simplest possible diamond (a divergence point, two nodes, and a convergence point), we were able to test that the real failure probability of the topology, which is 0.03125, given the set of n_k values used by the MDA for a failure probability of 0.05, was respected. We ran the MDA 1000 times on this topology to obtain a sample mean rate of failure, and obtained 50 such samples to obtain an overall mean and a confidence interval. This took 10 minutes on a contemporary laptop machine, giving a 0.03206 mean of failure, with a 95% confidence interval of size 0.00156. We were able to run the same test on much larger topologies as well, as indicated in the previous section. Fakeroute is available as free open-source software at the URL mentioned at the end of Sec. 1.

4 MULTILEVEL ROUTE TRACING

The third principal contribution of this paper, after the MDA-Lite and Fakeroute of the previous sections, is IPv4 multilevel route tracing, embodied in a version of Paris Traceroute that we refer to here as Multilevel MDA-Lite Paris Traceroute (MMLPT). By "multilevel", we mean that the tool provides router-level information in addition to the standard interface-level information. Some router-level information is already commonly provided by standard Traceroute command line tools, as they perform DNS look-ups on the IP addresses that they discover, and the name of an interface is often a variant on the name that has been assigned to the router as a whole. In addition, some of the prior work [20, 46] that we describe in Sec. 6 can reveal router or middlebox level information in the context of a Traceroute. Within the network measurement community, there are survey workflows, such as the one employed by bdrmap [35], that perform route traces and then alias resolution, and there are survey tools, such as scamper [34], that are capable

of performing both functions independently. To take another recent example, Marchetta et al. [37], employed a specialized tool, Paris Traceroute with the MDA, to conduct multipath tracing, and then another specialized tool, MIDAR, to conduct alias resolution on the IP addresses that the first tool reveals. But there has not previously been a command-line Traceroute tool, in the line of Van Jacobson's Traceroute [31], Modern Traceroute for Linux [12], and the like, with an option to obtain a router level view of multipath routes. With the advent of multipath route tracing ten years ago, it would seem to be a natural next step to incorporate alias resolution directly into Traceroute itself. Such a tool could readily be slotted in to workflows that currently invoke a Traceroute, and it would bring new capabilities to those, such as network operators, who use Traceroute for network troubleshooting purposes.

Alias resolution from a Traceroute perspective, coming as it does from a single route trace from a single vantage point, will never be as complete as alias resolution performed from multiple vantage points on IP addresses gleaned from traces from multiple vantage points. Nevertheless, we argue, alias resolution integrated into Traceroute, provides valuable information. When one observes multiple parallel paths in a route trace, the question immediately arises as to whether they are independent or not. Between two adjacent hops, one could be observing links to different interfaces on a single router or links to separate routers. MMLPT provides the capacity to distinguish between these cases at the moment of the route trace, without having to apply an additional tool for post hoc analysis, such Marchetta et al in [37]. Anyone who conducts route traces outside of the context of a dedicated survey, such as a network operator performing troubleshooting, can benefit.

The remainder of this section describes the alias resolution techniques that MMLPT employs (Sec. 4.1) and shows how we evaluate them (Sec. 4.2). Survey results using the tool are reported in Sec. 5.2.

4.1 Alias resolution

As mentioned in the Related Work section, MMLPT performs alias resolution using MIDAR's Monotonic Bounds Test (MBT) [33] and two techniques described by Vanaubel et al.: Network Fingerprinting [46], and MPLS Labeling [45]. In its overall approach, it follows the MBT's set-based schema for alias identification. An initial set is established of all of the candidate addresses, and then broken down into smaller and smaller sets as probing evidence indicates that certain pairs of addresses are not related. The sets are composed in such a way that each address in a set has failed alias tests with every address in every other set. At any point, each set that contains two or more addresses is considered to consist of the aliases of a common router. Further probing further refines these sets.

MIDAR faces a particular challenge in establishing its initial sets of candidate aliases, as it is designed to seek aliases from on the order of a million candidate addresses. It breaks this large number down into manageable sized initial sets by sorting aliases on the basis of how fast their IP IDs are evolving over time. MMLPT skips this step, as its task is narrower: to seek aliases among the addresses found in a single multipath route trace. It assumes that the aliases of a given router are to be found among the addresses found at a given hop, and so there will be at most on the order of one hundred

candidate aliases. As a result, we only borrow the MBT from MIDAR, and not its full complement of probing stages and heuristics.

Evidence that two addresses are not related comes in different forms, depending upon the test:

- The MBT looks at sequences of IP IDs from addresses that have been probed alternately. A monotonic increase in identifiers, taking wraparound into account, is consistent with the addresses being aliases, whereas a single out-of-sequence identifier is used to place the addresses into separate alias sets. We recall that MMLPT has used UDP indirect probing and that we have used MIDAR with UDP, TCP, and ICMP direct probing to collect IP ID time series.
- Network Fingerprinting looks at the TTLs of reply packets to a ping style probe and a Traceroute style probe, and infers their likely initial TTLs. Replies to probes of different addresses having different initial TTLs are almost certainly from different routers, and so the addresses are placed into separate alias sets.
- MPLS Labeling looks at the MPLS labels that appear in reply packets from different addresses. Vanaubel et al. [45] have characterized the different cases of MPLS tunnels with load balancing and developed methods to infer aliases from MPLS labels. To be usable, labels of interfaces in an MPLS tunnel have to be constant over time for each interface. Otherwise, MPLS labels are not helpful to infer aliases. Then, if, for two interfaces in an MPLS tunnel found at the same hop, their labels differ, it is highly likely that these two interfaces belong to two different routers. So the addresses are placed into separate alias sets. Conversely, if the labels are the same for the two interfaces, then it is highly likely that these two interfaces belong to the same router.

False positives, in which two addresses that are not aliases remain in the same set, can arise through their routers having identical fingerprints and MPLS signatures (when available), alongside a lack of sufficient MBT probing. False negatives, in which two addresses that are in fact aliases get placed in separate sets can arise when, instead of a single router-wide IP ID counter, a router employs separate IP ID counters for each flow identifier, and so the addresses fail the MBT [24].

Some of the basic data required by these techniques is collected as part of basic MDA-Lite Paris Traceroute probing: IP IDs that are used by the MBT; the TTLs of "indirect probing" reply packets that are used by Network Fingerprinting; and the MPLS labels that appear in reply packets. A light version of the MBT, along with MPLS Labeling, can therefore be performed "for free", based on these data. The results are then refined by MMLPT over additional rounds of probing, with the direct probes required for Network Fingerprinting and indirect probes to solicit more and longer sequences of IP IDs for the MBT. The signature-based methods are applied just once, whereas successive rounds of the MBT refine the results. After 10 rounds, MMLPT declares sets that remain as aliases.

Our tool, like MIDAR, produces three possible outcomes for a pair of IP addresses. Either it accepts that they are aliases of the same router, or they are rejected as being aliases of the same router, or it is not possible for the tool to determine one way or the other. Failure
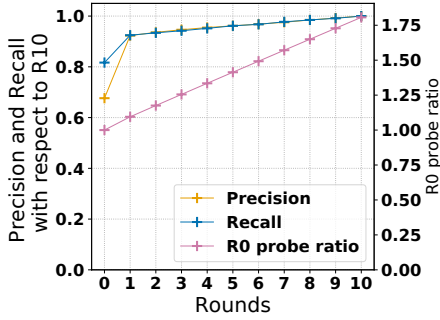
Figure 5: Alias resolution over ten rounds

to determine is not an unusual case, as there are addresses from which responses to probes do not have monotonically increasing IP ID values. Such an address might, for instance, systematically respond with the same value in response to every probe. Or it might not provide a sufficient number of responses from which to construct a time series.

4.2 Evaluation

We looked at how MMLPT's alias resolution results evolve round by round. Round 0 is based on just the data obtained through MDA-Lite Paris Traceroute, with no additional probing. The MBT and signature-based tests are applied to the extent possible. Round 1 adds one direct probe to each of the IP addresses at a given hop, in order to provide more complete Network Fingerprinting signatures. It also is the first round of MBT probing, attempting to elicit 30 replies per address. Each subsequent round through to Round 10 consists of an additional 30 indirect probes per address, in order to further refine the alias sets using the MBT.

Fig. 5 presents overall values for precision, recall, and numbers of probes sent over the 10,000 measurements conducted for the MDA-Lite evaluation of Sec. 2.4. We do not have ground truth, so precision and recall are relative to our best available determination of the alias sets, which is the result of Round 10 in each case. The number of probes is relative to the number sent in Round 0.

Round 0, with no probing beyond that which is performed for MDA-Lite Paris Traceroute, yielded 68% precision and 81% recall with respect to the Round 10 results. A significant jump to 92% in both cases came with a first round of probing, and then there was a slow increase with each successive round. The additional probing for each round was less than 10% of the basic MDA-Lite Paris Traceroute probing.

These results indicate that we can glean router-level information with a modest amount of additional probing, typically 20% more is enough to get a precision and a recall greater than 92% with respect to round 10, and 75% more to complete the ten rounds. Additional work will be required in order to better establish a firm basis against which to compare, so as to provide clearer guidance on the tradeoff between probing and the completeness and accuracy of the results.

We also looked at the potential benefits and costs of adding direct probing, as we had implemented MMLPT with only indirect probing, for the MBT. For each diamond, MMLPT identifies zero or more address sets as routers, validating or rejecting address sets

	Accept Direct	Reject Direct	Unable Direct
Accept Indirect	0.365	0.005	0.283
Reject Indirect	0.144	N/A	N/A
Unable Indirect	0.203	N/A	N/A

Table 2: Findings for 4798 address sets identified as routers either by indirect probing (MMLPT) or direct probing (MIDAR), expressed as portions adding up to 1.0

via indirect probing. We compare these results with what direct probing IP ID techniques would have found, using MIDAR for this. We ran MIDAR on all the addresses of the diamond, and MIDAR too identifies zero or more address sets as routers in the diamond. We take the union of the address sets identified by both tools, and compare: which ones did both accept as being a router, and which ones were accepted by one of the tools but not by the other? If a tool does not accept an address set, it is either because it has rejected it (for instance by finding a pair of addresses that has failed the MBT) or because it is unable to determine if one or more of the addresses belongs in the set (for instance because of an insufficient time series from an address).

Table 2 shows the results for 4798 address sets, of which 3414 were identified as routers by MIDAR and 3140 by MMLPT. The values are the portion of address sets that fall within each category. 36.5% were accepted as routers by both MIDAR and MMLPT. Just 0.5% of sets accepted by MMLPT are rejected by MIDAR, whereas 14.4% of sets accepted by MIDAR are rejected by MMLPT. The latter can be explained by routers that implement per-interface counters for the IP ID for the ICMP Time Exceeded messages associated with indirect probing and router-wide counters for the ICMP Echo Reply messages associated with direct probing.

Significant portions of sets accepted by one tool encounter a failure to determine a result by the other tool: 20.3% of sets accepted by MIDAR led to no conclusion by MMLPT and 28.3% of sets accepted by MMLPT led to no conclusion by MIDAR. Upon further investigation, we found that 98.6% of the non conclusive cases for MMLPT are due to either constant (mostly zero) IP IDs and 1.4% to non monotonic IP ID series. Looking at MIDAR logs, we found that the 28.3% inconclusive cases had different causes: for each inconclusive set, at least one IP in the set was either unresponsive to direct probing (60.5%), or its IP ID series was a copy of the probe IP ID (22.8%), or its IP ID series was non monotonic (13.6%), or MIDAR got unexpected responses, meaning that the reply did not match that which would be expected based upon the probe protocol used (3.1%).

Our overall conclusion is that direct probing provides a potentially valuable complement to indirect probing, and that we should include it in future versions of MMLPT, while also evaluating the tradeoff in what is gained against the additional probing cost that it will entail.

5 SURVEYS

This section presents the two surveys that we have conducted, one at the IP level, the other at the router level. The aim in both is to characterize the topologies that are encountered by multipath route

tracing in the IPv4 Internet, along the lines of earlier surveys [14, 19, 37] mentioned in the Related Work section.

Our focus is on the "diamonds" (see Sec. 2.1 for the definition) that are encountered in a route trace. We define a a **distinct diamond** by its divergence point and its convergence point. This means that if a diamond is encountered multiple times in the course of a survey, there might be differences in its measured internal topology from one encounter to the next. If either a divergence point or a convergence point is non-responsive (a "star" in common parlance), we consider it as different from a diamond that has responsive divergence and convergence points, even if the two diamonds have other IP addresses in common. Since a diamond might show up in multiple measurements, we define each encounter with a distinct diamond to be a **measured diamond**. Each way of counting reflects a different view of what is important to consider: the number of such topologies, or the likelihood of encountering one. We look at both.

The surveys describe how large diamonds are, both in number of hops and in number of vertices at a given hop. Also, because we have found that "uniformity" and "meshing" are relevant to the ability to economize on probes when tracing at the IP level (see Sec. 2.2), we describe these features. For the metric definitions that follow, we apply those of Augustin et al. [19] for "maximum width" and "maximum length" and add "maximum width asymmetry" and "ratio of meshed hops". As illustrated in Fig. 6, these are:

The **maximum width** is the maximum number of vertices that can be found at a single hop, as in the boxed hop of the left-hand diamond.

The **maximum length** is the length of the longest path between the divergence and the convergence point, as shown by the set of bold edges in the left-hand diamond.

The **maximum width asymmetry** is a topological indicator of a lack of uniformity. We define it first for a pair of hops i and $i + 1$.

- If hop i has fewer vertices than hop $i + 1$, it is the maximum difference in the number of successors between two vertices at hop i.
- If hop i has more vertices than hop $i + 1$, it is the maximum difference in the number of predecessors between two vertices at hop $i + 1$.
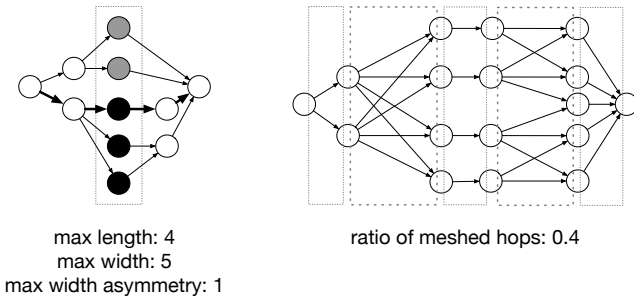- If hops i and $i + 1$ have identical numbers of vertices, it is the maximum of the two values described above.

For a diamond as a whole, it is the largest value of maximum width asymmetry found across all hop pairs, as shown by the grey and black vertices of the left-hand diamond.

The **ratio of meshed hops** of a diamond is the portion of hop pairs of hops that are meshed, as shown in the right-hand diamond, in which two of the five hop pairs are meshed, for a ratio of 0.4.

5.1 IP level survey

The IP level survey is based on multipath route traces from 35 sources towards 350,000 destinations during two weeks starting 8 March 2018.

The route tracing tool was the *libparistraceroute*-based MDA Paris Traceroute [7], using its default parameters. We employed UDP probes, as Luckie et al. [36] found best results for discovering load balanced paths with such probes.

The sources were PlanetLab nodes running Fedora 24 or 25, obtained through PlanetLab Europe [10]. (We also ran a survey with similar results, which can be found at the URL mentioned at the end of Sec. 1, on the new EdgeNet infrastructure [3] affiliated with PlanetLab Europe.)

The destinations were chosen at random from the IPv4 addresses rated as "highly responsive" in the Internet Address Hitlist Impact dataset `Internet_address_hitlist_it78w-20171113`, ID DS-822, covering 17 January 2015 to 15 December 2017 [13].

We discarded route traces that we could not collect because of infrastructure troubles, yielding 294,832 exploitable results, among which 155,030 passed through at least one per-flow load balancer. There were 60,921 distinct and 220,193 measured diamonds.
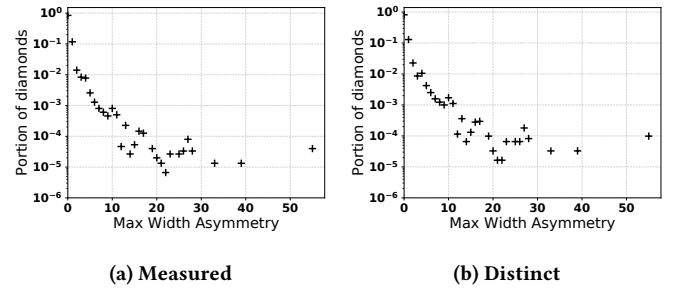
(a) Measured   **(b) Distinct**

Figure 7: Width asymmetry

max length: 4
max width: 5
max width asymmetry: 1

ratio of meshed hops: 0.4

Figure 6: Diamond metrics
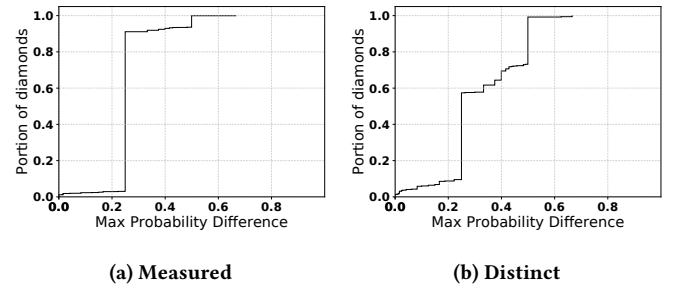
(a) Measured   **(b) Distinct**

Figure 8: Maximum probability difference in width-asymmetric diamonds

We start by looking at uniformity and meshing.

Uniformity. In both measured and distinct diamond asymmetry distributions (Fig. 7), 89% of diamonds have zero asymmetry. This means that most diamonds are uniform, provided that load balancing is uniform across next hop interfaces, and supports the MDA-Lite's assumption of uniformity. But if the MDA-Lite cannot detect the asymmetry in a diamond that is among the 11% that are asymmetric, it will not switch over to the full MDA and it risks failing to discover the full topology. It is most likely to encounter difficulty on an unmeshed diamond, as, when meshing is detected, the full MDA is invoked. Only 2.3% of measured and 3.6% of distinct diamonds are both asymmetric and unmeshed. We examined these diamonds for differences in discovery probability among vertices at a common hop, plotting the CDFs of all non-zero probability differences in Fig. 8. In these cases, 90% of measured and 58% of distinct diamonds have a maximum probability difference of 0.25 and, for both, 99% have a maximum probability difference of 0.5. This indicates that the MDA-Lite is very unlikely to fail in uncovering a lack of uniformity, which is borne out by our experimental results in Sec. 2.4. This issue could be more rigorously studied with further mathematical analysis.
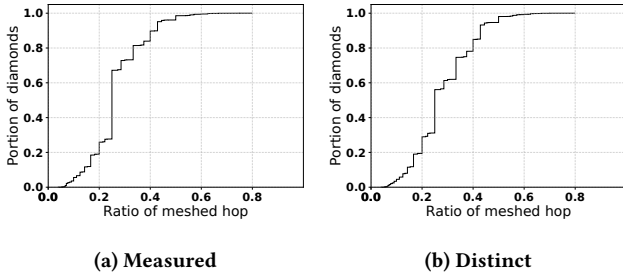

(a) Measured   **(b) Distinct**

Figure 9: Ratio of meshed hops

Meshing. Of the 220,193 measured diamonds in our survey, 32,430 present at least one meshed hop, and of the 60,921 distinct diamonds, 19,138 are meshed. Fig. 9 plots CDFs of the ratio of meshed hops for the meshed diamonds. The MDA-Lite offers probe savings over the full MDA when a pair of hops is not meshed. More than 80% of meshed diamonds have a ratio of of meshed hops under 0.4, which indicates a significant potential for the MDA-Lite to realize significant probe savings, even on meshed diamonds. We continue by looking at the length and width metrics, for which the distributions are shown in Fig. 10. Almost half of both measured and distinct diamonds have a maximum length of 2, meaning that they consist of a divergence point, a single multi-vertex hop, and a convergence point. The MDA-Lite is more economical than the full MDA on such diamonds. The largest value of maximum width encountered is 96. Such a high value is unprecedented, with earlier surveys [19, 37] reporting maximum widths of at most 16. A notable feature of the maximum width distributions is their peaks at 48 and 56. Further investigation indicates that the distinct diamond distribution might be overstating what is in fact being encountered by the route traces. Though the diamonds are distinct by our definition, meaning that they have a unique pair of divergence and convergence points, they
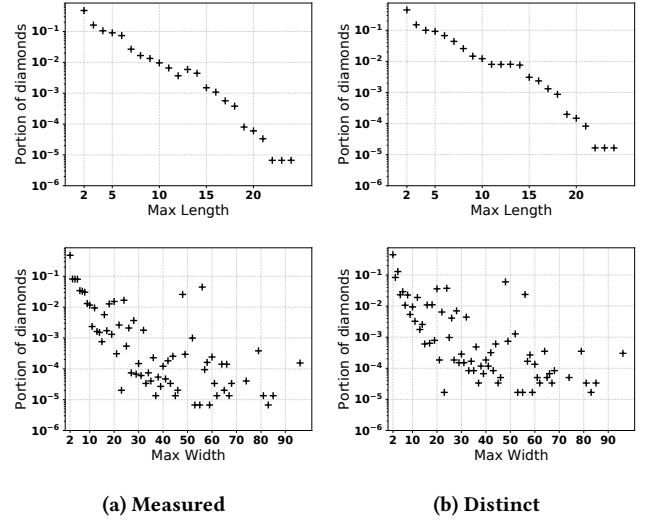

(a) Measured   **(b) Distinct**

Figure 10: Maximum length and maximum width

share a large portion of their IP addresses. This suggests a common structure that is being frequently encountered via a variety of ingress points.
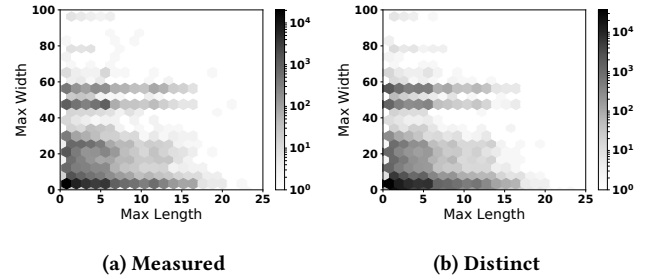

(a) Measured   **(b) Distinct**

Figure 11: Maximum length and maximum width joint distributions

Looking at the joint distributions of maximum width and maximum length (Fig. 11), we see that short and narrow diamonds continue to be the most common, as found in previous surveys. For example, we found that 24.2% of measured and 27.4% of distinct diamonds were of maximum length 2 and maximum width 2, corresponding to the simplest possible diamond. The maximum width 48 and 56 diamonds also reveal themselves to have a variety of different maximum lengths.

5.2 Router level survey

The router level survey is based upon the 155,030 route traces from the IP level survey that passed through at least one load balancer. We retraced these with Mutilevel MDA-Lite Paris Traceroute during two weeks, starting on 3 April 2018. For each trace, we obtained IP level output and router level output.

We found 646 cases of distinct address sets (0.98% of the total alias set) that were considered as aliases by one measurement, but
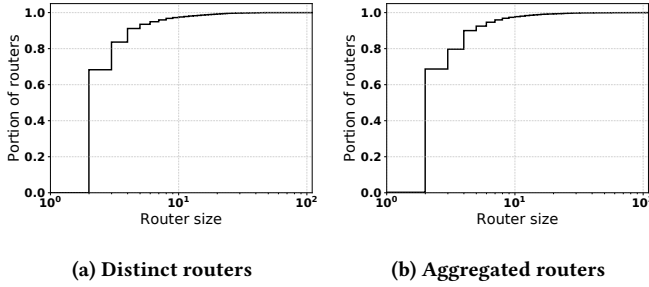
(a) Distinct routers

(b) Aggregated routers

Figure 12: Router size

(a) IP level

(b) Router level

Figure 13: Maximum width of unique diamonds

Case	Fraction
No change	0.579
Single smaller diamond	0.355
Multiple smaller diamonds	0.006
One path (no diamond)	0.058

Table 3: Effect of alias resolution on unique diamonds

Figure 14: Joint distribution of maximum width before and after alias resolution

discarded or not found by another, although they had both seen the entire address set at the IP level. A deeper analysis showed that 295 of those cases were due to a constant 0 IP ID series collected by one measurement for at least one address in the address set, whereas the other measurement could build a monotonic IP ID time series for each of the addresses in the address set. The remaining 351 cases were false positives, which were then discarded from the router dataset analysed in this section.

We looked at what we term the "size" of the routers that were found, the size being the number of IP interfaces identified as belonging to a router. A route trace from a given vantage point is bound to pick up mostly the ingress interfaces facing that point, which tend to be the ones from which it receives responses, and so this metric will be an underestimate of the true number of interfaces. We also aggregated the IP interface sets from multiple traces through transitive closure based upon two sets having at least one address in common, which may give less of an underestimate, but is still incomplete, as we do not perform full alias resolution on the overall IP addresses set found. CDFs of the sizes are shown in Fig. 12. 68% of the routers had a size of 2 and 97% had a size of 10 or less. We found 1 distinct router with more than 50 interfaces, and 5 such routers when we aggregated the address sets.

We looked at what happens to each IP level diamond when it is resolved into a router level diamond. There are four possibilities: (1) there is no alias resolution, so the diamond remains the same; (2) the diamond resolves into a single smaller diamond; (3) the diamond resolves into a series of smaller diamonds; (4) the diamond disappears completely, being resolved into a straight path of routers. As Table 3 shows, some degree of router resolution takes place on 41.9% of unique diamonds. In comparison, Marchetta et al. [37] saw, in 2016, a 33% reduction in diamond max-width, when applying MIDAR a posteriori to multipath route traces.
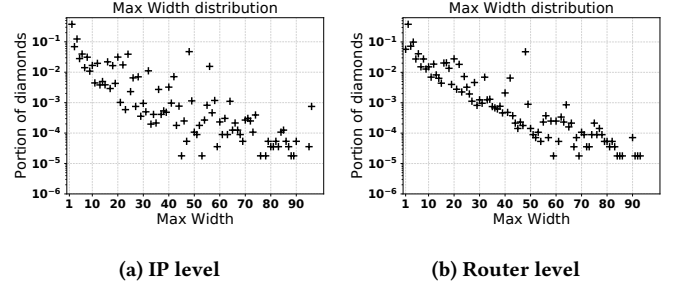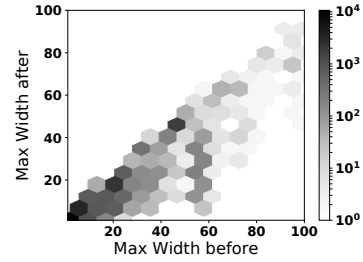
We looked at the effect of alias resolution on diamond width. Fig. 13 plots the distributions obtained by the MDA-Lite before and after alias resolution. We observe that the peak at maximum width 48 has remained, whereas the one at 56 has disappeared. On closer inspection, we find that the max width 56 diamond at the IP level resolved into several smaller diamonds at the router level. These router-level diamonds were of unaggregated sizes between 2 and 49 IPs.

Finally, we looked at width reduction diamond by diamond. Fig. 14 plots the joint distribution of maximum width before and after alias resolution of those diamonds that changed size. Large width reductions are rare, but do take place. The darker grey vertical series of values just to the left of 60 show the maximum width 56 diamonds being broken down into smaller diamonds at the router level.

6 RELATED WORK

6.1 Contributions

Our MDA-Lite and multilevel route tracing work builds directly on Paris Traceroute [15, 48] and the Multipath Detection Algorithm (MDA) [17, 47]. It also inscribes itself in the line of measurement work that has sought to improve our ability to trace the IP level paths that packets take through the Internet, such as Reverse Traceroute [32], which uses the IP Record Route option to learn IP addresses on the return path taken by probe replies; Vanaubel et al.'s Network Fingerprinting technique [46] for examining the TTLs of probe replies to determine which type of router might have sent them and, combined with examination of the MPLS label stack that is received in an ICMP Time Exceeded message, to trace a path's MPLS tunnels; or Dublin Traceroute [20], which uses

Steven Bellovin's technique [21] for examining the IP ID field of probe replies for NAT box detection in order to identify NAT boxes on a multipath route. Similarly to the latter two, our multilevel route tracing technique goes beyond the interface level to uncover information about the devices through which packets pass.

Our multilevel route tracing makes use of existing alias resolution techniques, notably MIDAR's [33] state of the art Monotonic Bounds Test (MBT) for comparing overlapping time series of the IP IDs of probe replies. The MBT itself builds on the pioneering approaches of Ally [44] and RadarGun [22]. We also use Vanaubel et al.'s Network Fingerprinting [46]. But there are other alias resolution techniques that we do not use. For instance, the Mercator [27] and iffinder [30] approach, which is based on Pansiot and Grad's technique [39] of seeing whether a probe to one IP address elicits a reply from another. Nor do we use Sherry et al.'s prespecified timestamp technique [41]. This is because we currently limit our Traceroute tool to Traceroute-style probing, what the MIDAR paper calls "indirect probing", that is based principally on TTL expiry, rather than Ping-style probing, otherwise called "direct probing". But there is no reason in principle, aside from additional overhead, why such techniques could not be added. We also do not use Spring et al.'s technique [43] of examining the names returned by reverse DNS look-ups and looking for similarities, as this requires hand-designed rules to reflect each Internet service provider's naming conventions. Nor do we use graph analysis based alias resolution techniques such as APAR [28], kapar [5], or DisCarte [42], as these work by analyzing route traces from multiple sources to multiple destinations.

Fakeroute is a network simulator purpose-built for one thing: statistical validation of multipath route detection algorithm implementations on a variety of topologies. As such, it does not implement any other features that general network simulators such as ns-3 [29], or emulators, such as GNS3 [4], that can run real router OSes, might offer.

The surveys follow on previous surveys of load balanced paths in the Internet. Our survey provides an update on Augustin et al.'s survey [19] from ten years ago. Like in Marchetta et al.'s survey [37], our survey transforms IP level traces into router-level topologies, but it does so with a single tool, while tracing, rather than with additional measurements by other tools a posteriori. Almeida et al. characterized multipath routes in the IPv6 Internet [14], while we have yet to extend our tool to do the same. Marchetta et al.'s and Almeida et al.'s surveys are quite recent, from 2016 and 2017 respectively, but they report only a maximum of 16 interfaces at a given hop, whereas our survey reveals up to 96.

6.2 Multipath route tracing on RIPE Atlas

RIPE Atlas, because of the resource constraints on its probe boxes, does not deploy the MDA. Nonetheless, a rudimentary form of MDA can be realized on the platform. Within a repeating route tracing measurement, a level of flow ID variation is permitted: up to 64 variations of what is termed the *Paris ID*. Measurements are generally scheduled conservatively, and so over the course of minutes or hours a probe box may cycle through 64 distinct Paris IDs in its traces towards a destination. This approach implies that RIPE Atlas is capable of discerning multiple forward paths

between a source and a destination. However, it does so in a manner that is not optimized, neither in terms of probe savings nor in terms of statistical guarantees. This has motivated our search for an improved reduced-overhead MDA.

7 CONCLUSION AND FUTURE WORK

This paper made four contributions related to Paris Traceroute, each of which can be developed further. (1) For MDA-Lite, the alternative to the Multipath Discovery Algorithm (MDA) that significantly reduces overhead while maintaining a low failure probability, we hope to deepen the mathematical analysis in order to determine significance levels for the results, as had been done for the MDA [47]. Also, the assumption of uniform load balancing, which we believe to hold in almost all cases, could be tested by a rigorous survey, and the algorithm adjusted, which we believe would be straightforward, to take into account uneven load balancing if necessary. (2) For Fakeroute, the simulator that enables validation of a multipath tracing software tool's adherence to its claimed failure probability bounds, we could extend it to simulate exceptions to the assumptions made by the MDA and MDA-Lite. Some assumptions, such as that every probe will receive a reply, often do not hold in practice. Indeed, ICMP rate limiting is one common cause of a lack of replies, and a simulator that takes rate limiting into account could help in designing an algorithm to probe in ways less likely to trigger rate limiting. Another extension might be to allow simulation of multilevel route tracing. (3) For multilevel multipath route tracing, which has provided, a router-level view of multipath routes, we continue to investigate the differences between direct and indirect probing for alias resolution. (4) For the surveys of multipath routing in the Internet, showing, among other things, that load balancing topologies have increased in size well beyond what has been previously reported as recently as 2016, we would like to repeat them, conducting at a larger scale some of the side-by-side comparisons of MDA and MDA-Lite that we have so far conducted only on a smaller scale. Overall, the work is currently entirely focused on IPv4 and can benefit from being applied to IPv6.

REFERENCES

[1] [n. d.]. Ark. Retrieved September 12, 2018 from https://www.caida.org/projects/ark/locations

[2] [n. d.]. C++ Mersenne Twister. Retrieved September 12, 2018 from http://www.cplusplus.com/reference/random/mt19937/

[3] [n. d.]. EdgeNet. Retrieved September 12, 2018 from http://edge-net.org/

[4] [n. d.]. GNS3 emulator. Retrieved September 12, 2018 from https://www.gns3.com

[5] [n. d.]. kapar. Retrieved September 12, 2018 from https://www.caida.org/tools/measurement/kapar/

[6] [n. d.]. libnetfilter-queue library, netfilter.org project. Retrieved September 12, 2018 from http://fr.netfilter.org

[7] [n. d.]. libparistraceroute library. Retrieved September 12, 2018 from https://github.com/libparistraceroute/libparistraceroute

[8] [n. d.]. libtins packet crafting and sniffing library. Retrieved September 12, 2018 from http://libtins.github.io

[9] [n. d.]. M-Lab. Retrieved September 12, 2018 from https://www.measurementlab.net

[10] [n. d.]. PlanetLab Europe. Retrieved September 12, 2018 from https://www.planet-lab.eu

[11] [n. d.]. RIPE Atlas. Retrieved September 12, 2018 from https://atlas.ripe.net

[12] [n. d.]. Traceroute for Linux. Retrieved September 12, 2018 from http://traceroute.sourceforge.net

[13] [n. d.]. USC/ISI ANT Datasets. Retrieved September 12, 2018 from https://ant.isi.edu/datasets/all.html

[14] Rafael Almeida, Osvaldo Fonseca, Elverton Fazzion, Dorgival Guedes, Wagner Meira, and Ítalo Cunha. 2017. A Characterization of Load Balancing on the IPv6 Internet. In *Proc. PAM '17*.

[15] Brice Augustin, Xavier Cuvellier, Benjamin Orgogozo, Fabien Viger, Timur Friedman, Matthieu Latapy, Clémence Magnien, and Renata Teixeira. 2006. Avoiding Traceroute Anomalies with Paris Traceroute. In *Proc. ACM IMC '06*.

[16] Brice Augustin, Timur Friedman, and Renata Teixeira. 2006. Exhaustive path tracing with Paris traceroute. In *Proc. ACM CoNEXT '07*.

[17] Brice Augustin, Timur Friedman, and Renata Teixeira. 2007. Measuring Load-balanced Paths in the Internet. In *Proc. IMC '07*.

[18] Brice Augustin, Timur Friedman, and Renata Teixeira. 2007. Multipath tracing with Paris traceroute. In *Proc. E2EMON '07*.

[19] Brice Augustin, Timur Friedman, and Renata Teixeira. 2011. Measuring Multipath Routing in the Internet. *IEEE/ACM Trans. Netw.* 19, 3 (June 2011), 830–840.

[20] Andrea Barbeiro. 2016. Visualizing Multipath Networks with Dublin Traceroute. Presentation at the MOCA Italian hacker camp.

[21] Steven M. Bellovin. 2002. A Technique for Counting NATted Hosts. In *Proc. IMW '02*.

[22] Adam Bender, Rob Sherwood, and Neil Spring. 2008. Fixing Ally's Growing Pains with Velocity Modeling. In *Proc. ACM IMC '08*.

[23] Ya Chang and Peter Boothe. 2018. A better schema for paris-traceroute. Presentation at AIMS '18 CAIDA Workshop.

[24] Weifeng Chen, Yong Huang, Bruno F Ribeiro, Kyoungwon Suh, Honggang Zhang, Edmundo de Souza e Silva, Jim Kurose, and Don Towsley. 2005. Exploiting the IPID field to infer network path and end-system characteristics. In *Proc. PAM '05*.

[25] Constantine Dovrolis, Krishna Gummadi, Aleksandar Kuzmanovic, and Sascha D Meinrath. 2010. Measurement lab: Overview and an invitation to the research community. *ACM SIGCOMM Comput. Commun. Rev.* 40, 3 (2010), 53–56.

[26] Marco Ferrante and Monica Saltalamacchia. 2014. The coupon collector's problem. *MATerials MATemàtics* 2014, 2 (May 2014), 1–35.

[27] Ramesh Govindan and Hongsuda Tangmunarunkit. 2000. Heuristics for Internet map discovery. In *Proc. IEEE Infocom 2000*.

[28] Mehmet H. Gunes and Kamil Sarac. 2009. Resolving IP Aliases in Building Traceroute-based Internet Maps. *IEEE/ACM Trans. Netw.* 17, 6 (Dec. 2009), 1738–1751.

[29] Thomas R. Henderson, Sumit Roy, Sally Floyd, and George F. Riley. 2006. ns-3 Project Goals. In *Proc. WNS2 '06*.

[30] Bradley Huffaker, Daniel Plummer, David Moore, and kc claffy. 2002. Topology discovery by active probing. In *Proc. '02 SAINT Workshops*.

[31] Van Jacobson. 1988. 4BSD routing diagnostic tool available for ftp. Email 8812201313.AA03127@helios.ee.lbl.gov to the IETF and end2end-interest e-mail lists.

[32] Ethan Katz-Bassett, Harsha V Madhyastha, Vijay Kumar Adhikari, Colin Scott, Justine Sherry, Peter Van Wesep, Thomas E Anderson, and Arvind Krishnamurthy. 2010. Reverse traceroute.. In *Proc. NSDI '10*.

[33] Ken Keys, Young Hyun, Matthew Luckie, and kc claffy. 2013. Internet-Scale IPv4 Alias Resolution with MIDAR. *IEEE/ACM Trans. Netw.* 21, 2 (Apr 2013), 383–399.

[34] Matthew Luckie. 2010. Scamper: a scalable and extensible packet prober for active measurement of the internet. In *Proc. ACM IMC '10*.

[35] Matthew Luckie, Amogh Dhamdhere, Bradley Huffaker, David Clark, et al. 2016. bdrmap: inference of borders between IP networks. In *Proc. ACM IMC '16*.

[36] Matthew Luckie, Young Hyun, and Bradley Huffaker. 2008. Traceroute Probe Method and Forward IP Path Inference. In *Proc. ACM IMC '08*.

[37] Pietro Marchetta, Antonio Montieri, Valerio Persico, Antonio Pescapé, Ítalo Cunha, and Ethan Katz-Bassett. 2016. How and how much traceroute confuses our understanding of network paths. In *Proc. LANMAN '16*.

[38] Donald J. Newman. 1960. The Double Dixie Cup Problem. *The American Mathematical Monthly* 67, 1 (1960), 58–61.

[39] Jean-Jacques Pansiot and Dominique Grad. 1998. On Routes and Multicast Trees in the Internet. *ACM SIGCOMM Comput. Commun. Rev.* 28, 1 (Jan. 1998), 41–50.

[40] RIPE NCC Staff. 2015. RIPE Atlas. *Internet Protocol Journal* 18, 3 (2015).

[41] Justine Sherry, Ethan Katz-Bassett, Mary Pimenova, Harsha V. Madhyastha, Thomas Anderson, and Arvind Krishnamurthy. 2010. Resolving IP Aliases with Prespecified Timestamps. In *Proc. ACM IMC '10*.

[42] Rob Sherwood, Adam Bender, and Neil Spring. 2008. Discarte: A Disjunctive Internet Cartographer. *ACM SIGCOMM Comput. Commun. Rev.* 38, 4 (Aug. 2008), 303–314.

[43] Neil Spring, Mira Dontcheva, Maya Rodrig, and David Wetherall. 2004. *How to Resolve IP Aliases*. Technical Report 04-05-04. University of Washington, Computer Science and Engineering.

[44] Neil Spring, Ratul Mahajan, and David Wetherall. 2002. Measuring ISP Topologies with Rocketfuel. *ACM SIGCOMM Comput. Commun. Rev.* 32, 4 (Aug. 2002), 133–145.

[45] Yves Vanaubel, Pascal Mérindol, Jean-Jacques Pansiot, and Benoit Donnet. 2015. MPLS Under the Microscope: Revealing Actual Transit Path Diversity. In *Proc. ACM IMC '15*.

[46] Yves Vanaubel, Jean-Jacques Pansiot, Pascal Mérindol, and Benoit Donnet. 2013. Network Fingerprinting: TTL-based Router Signatures. In *Proc. ACM IMC '13*.

[47] Darryl Veitch, Brice Augustin, Renata Teixeira, and Timur Friedman. 2009. Failure Control in Multipath Route Tracing. In *Proc. IEEE Infocom '09*.

[48] Fabien Viger, Brice Augustin, Xavier Cuvellier, Clémence Magnien, Matthieu Latapy, Timur Friedman, and Renata Teixeira. 2008. Detection, understanding, and prevention of traceroute measurement artifacts. *Computer Networks* 52, 5 (April 2008), 998–1018.